Nanotechnology

PURPOSE-LED PUBLISHING™

Coupling of single nanodiamonds hosting SiV color centers to plasmonic double bowtie microantennas

To cite this article before publication: Sarah Lindner *et al* 2025 *Nanotechnology* in press https://doi.org/10.1088/1361-6528/ada9a4

Coupling of single nanodiamonds hosting SiV color centers to plasmonic double bowtie microantennas

S. Lindner[1,2,†,*], N. Rahbany[3,4,†], C. Pauly[5], L. Gines[6,7], S. Mandal[6], O. A. Williams[6], A. Muzha[8], A. Krueger[8,9], R. Bachelot[3], C. Couteau[3], and C. Becher[1]

[1]Fachrichtung Physik, Universität des Saarlandes, Campus Geb. E2.6, 66123 Saarbrücken, Germany
[2]Institut für Physik, Karl-Franzens-Universität Graz, Universitätsplatz 5, 8010 Graz, Austria
[3]Light, Nanomaterials and Nanotechnologies Laboratory (L2n), Université de Technologie de Troyes and CNRS UMR7076, 12 rue Marie Curie, 10004 Troyes Cedex, France
[4]Department of Physics and Astronomy, Faculty of Natural and Applied Sciences, Notre Dame University-Louaize, P.O. Box 72, Zouk Mosbeh, Lebanon
[5]Lehrstuhl für Funktionswerkstoffe, Universität des Saarlandes, Campus Geb. D3 3, 66123 Saarbrücken, Germany
[6]School of Physics and Astronomy, Cardiff University,The Parade, Cardiff CF24 3AA, United Kingdom
[7]Fysikum, Stockholm University, Roslagstullsbacken 21, 106 91 Stockholm, Sweden
[8]Institut für Organische Chemie, Universität Würzburg, Am Hubland, 97074 Würzburg, Germany
[9]Institute of Organic Chemistry, University of Stuttgart, Pfaffenwaldring 55, 70569 Stuttgart, Germany
[†]These authors contributed equally to this work
[*]Author to whom any correspondence should be addressed: sarah.lindner@uni-graz.at

November 18, 2024

Abstract

Color centers are promising single-photon emitters owing to their operation at room temperature and high photostability. In particular, using

nanodiamonds as a host material is of interest for sensing and metrology. Furthermore, being a solid-state system allows for incorporation to photonic systems to tune both the emission intensity and photoluminescence spectrum and therefore adapt the individual color center to desired properties. We show successful coupling of a single nanodiamond hosting silicon-vacancy color centers to a plasmonic double bowtie antenna structure. To predict the spectrum of the coupled system, the photoluminescence spectrum of the SiV centers was measured before the coupling process and convoluted with the antenna resonance spectrum. After transferring the nanodiamond to the antenna the combined spectrum was measured again. The measurement agrees well with the calculated prediction of the coupled system and therefore confirms successful coupling.

Keywords: Silicon-vacancy center, color center, nanodiamond, Pick and Place Technique, plasmonic antenna

1 Introduction

Color centers in diamond are being widely used as efficient single photon sources due to emission of indistinguishable photons and photostability at room temperature. This allows them to play an important role in the fields of quantum information processing [1, 2, 3, 4, 5, 6], super-resolution microscopy [7, 8, 9], biological imaging [3, 9, 10], nanoscale sensing [9, 11] and quantum metrology [12]. Silicon vacancy (SiV) centers in diamond have shown to have several advantages over other types of defects owing to their strong and narrow-band fluorescence spectrum at room temperature[13] (silicon-vacancy center in bulk diamond: FWHM 5 nm at a center wavelength of 737 nm) with low phonon coupling, a short lifetime (1 ns), an optically accessible spin[14] and an almost fully linearly polarized zero phonon line fluorescence [15]. However, the reported values of the photoluminescence (PL) of SiV centers vary considerably and their radiative quantum efficiency so far remains low[16]. Consequently, experiments involving coupling SiV centers to optical cavities have led to an improvement in their radiative quantum efficiency and Purcell factor, as well as a reduction in lifetime [17, 18, 19, 20, 21, 22]. Plasmonic coupling, which in general allows for high local field confinement, was also studied to enhance the emission of SiV centers in the vicinity of metal nanoparticles[23, 24, 25, 26], in hybrid metal-diamond structures[27, 28, 29, 30], and in plasmonic antennas [31, 32]. In this work, we present the integration of SiV centers in nanodiamonds with plasmonic double bowtie microantenna structures. A single nanodiamond hosting SiV centers is pre-characterized and transferred to the gap of a gold microantenna by the "pick-and-place" technique with the help of a nanomanipulator[33, 34]. We show that the PL spectrum of the nanodiamond is modified depending on the geometry of the plasmonic antenna. This provides us with flexibility in designing the antennas to accurately predict and shape the emitters' PL spectrum as desired.

2 Nanodiamond Characterization – Photoluminescence Spectroscopy

A solution of nanodiamonds with an average diameter of 100 nm was spin-coated on a clean iridium substrate[35, 36]. To ensure that a pre-characterized nanodiamond exhibiting the desired optical properties (i.e. narrow linewidth and high count rate) can be located again for the pick-and-place fabrication step, the iridium substrate was engraved with reference cross markers produced by a focused ion beam prior to the spin-coating process. The nanodiamonds were produced by milling a diamond film grown by chemical vapor deposition. The nanocrystalline diamond starting material was directly grown on a silicon wafer. A microwave hydrogen plasma containing 1% methane was used to grow on purified 5 nm nanodiamond seeds (produced by PlasmaChem). To induce in-situ SiV center creation, sacrificial silicon pieces are situated in the growth chamber. The diamond is then milled by a wet-milling process in a vibrational mill with steel beads to crystals of average diameter of 100 nm. The milling was followed by an etching and oxidative treatment using concentrated HCl and subsequently HNO_3/H_2SO_4 1:1 in order to remove any debris from the milling process and homogenize the surface to carry an oxygen-termination. Further details are reported in [36]. The particle size was determined with laser diffraction spectroscopy. After spin-coating, the sample was placed in an ovenat atmospheric conditions for 3 hours at 450 °C to oxidize the surface and remove any residual graphite and amorphous carbon. In a first step, we identified sufficiently isolated nanodiamonds suited for pick-and-place handling to the antenna structure. For that purpose, we recorded high resolution images of the sample surface with a commercial confocal laser scanning microscope (Figure 1a). Next, the samples were tested in a home-built confocal microscopy setup to identify nanodiamonds hosting SiV centers with the preferred optical properties, such as narrow linewidth and high count rate emission. In this setup, the sample is either illuminated with diffuse white light to investigate the sample surface, or with a red diode laser (Schaefter-Kirchhoff, $\lambda_{ex} = 660$ nm) that is focused onto the sample by a microscope objective (100x, NA = 0.8) to study the fluorescence of SiV centers in diamond. The same microscope objective collects light originating from the sample. The collected light can be guided to a CCD camera to image the sample surface; as well as to avalanche photo diodes (APDs) or a spectrometer to investigate the photoluminescence. Figure 1b shows a picture of the sample surface under white light illumination. White spots correspond to nanodiamonds that might contain SiV centers. They appear as bright spots due to the scattering caused by the white light illumination. The two bright lines correspond to two cross-shaped markers that were previously engraved on the surface of the sample as references for locating specific nanodiamonds later on. In order to test the presence of SiV centers in the nanodiamonds and to pre-select nanodiamonds hosting SiV centers with desired optical properties, the sample is excited with a laser and PL scans and spectra are recorded. A long pass filter ($\lambda = 720$ nm) is placed in the detection path to suppress excitation light from the laser. During the PL scan, the laser spot scans the surface and the emitted PL is recorded by the APD. The center wavelength of the zero-phonon line of an ideal

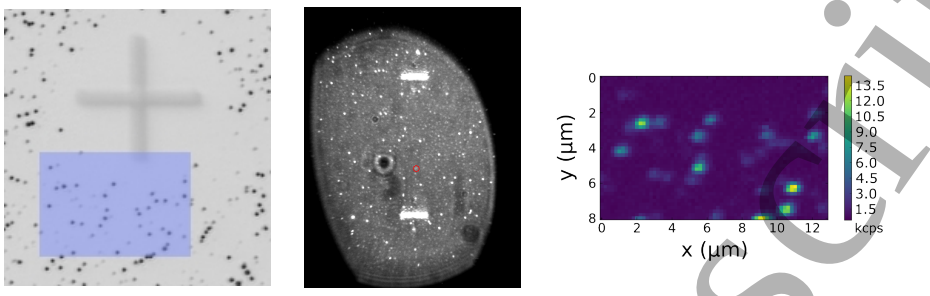

(a) (b) (c)

Figure 1: (a): Image recorded with a commercial high resolution laser scanning microscope. The area shaded in blue in corresponds to the area scanned for a PL signal shown in (c). (b): Dark field images of the sample surface of 100 nm nanodiamonds spin-coated on an iridium substrate illuminated with diffuse white light. The white bars are part of cross-shaped markers, which help to localize the selected nanodiamonds later. The white dots are nanodiamonds, while big black spots are artifacts. (c) Photoluminescence scan of a 8×13 µm^2 area on the sample. Bright dots correspond to nanodiamonds that might contain SiV centers.

SiV center is located at 738 nm. Due to strain in the diamond lattice, the center wavelength may shift [36]. Accordingly, we detect fluorescence in the spectral range 730 nm to 750 nm by inserting a bandpass filter in front of the APDs. Thus if a nanodiamond contains a SiV center, its emission will result in a bright spot in the PL scan. Figure 1c shows an example of a PL scan where bright spots (highlighted by the red circles) correspond to nanodiamonds that act as potential candidates for hosting SiV centers. To further verify the presence of SiV centers, also PL spectra are recorded at room temperature. As seen exemplarily in Figure 2, the intense narrow peak ($\lambda = 739.70\,\text{nm} \pm 0.02\,\text{nm}$, $\Delta\lambda = 9.5\,\text{nm} \pm 0.1\,\text{nm}$) in the spectrum correlates well with the ZPL of the SiV center, and therefore allows us to deduce that the studied nanodiamond contains at least one SiV center.

3 Double Bowtie Microantennas - FDTD Numerical Simulation and Fabrication

Metallic nanoparticles and microantennas are commonly employed for creating regions of intense electromagnetic fields. Unlike single bowtie antennas, double bowtie antennas benefit of inducing dramatic electromagnetic field confinement in their gap without requiring illumination with a specific light polarization [37, 38, 39]. Despite the non-radiative losses in such plasmonic structures, they have shown to increase the fluorescence emission of emitters placed in their vicinity [40]. In general, a double bowtie antenna is a structure consisting of 4 individual triangles, as depicted in Figure 3a). For the experiment reported in this work, the design restraints on the antenna are twofold: First, the main goal is the enhancement of the photolu-

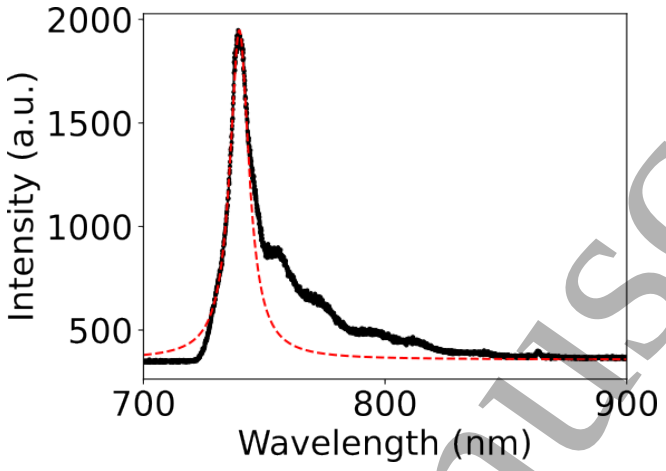

Figure 2: PL spectrum of a nanodiamond at room temperature. Black line: experimental results; red line: fit to experimental data, which yields the following values: ZPL center wavelength $\lambda = 739.70\,\text{nm} \pm 0.02\,\text{nm}$, linewidth $\Delta\lambda = 9.5\,\text{nm} \pm 0.1\,\text{nm}$

minescence of the zero-phonon line of the SiV center in a nanodiamnond (center wavelength $\sim 738\,\text{nm}$). Therefore, the antenna has to exhibit a resonant mode at around 738 nm. Second, the nanodiamond hosting an SiV center has to fit into the central gap between the antenna arms. The aforementioned nanodiamonds have a diameter of about 100 nm. Allowing for margins due to antenna production, exact nanodiamond size and the positioning process of the nanodiamond, the lower limit on the gap size amounts to 150 nm. Finite-difference time-domain (FDTD) simulations were performed using the Lumerical FDTD software package to characterize double bowtie antennas exhibiting various design parameters. Unlike a single bowtie that is sensitive to the polarization along its principal axis (C2 rotational symmetry) only, a double bowtie features a C4 rotational symmetry and therefore confines both parallel and perpendicular polarizations. For that, circularly polarized light with a wavelength range of $\lambda = 400\,\text{nm}$ to 1500 nm is chosen for illumination, which efficiently excites both the horizontal and vertical components of the structure. The optical properties of gold are taken from Palik [41], and the refractive index of the nanodiamond is chosen to be $n = 2.4$ at $\lambda = 660\,\text{nm}$[42]. The electric field intensity in the microantenna gap is then recorded numerically as a function of wavelength to identify the antenna resonance.

Antennas were made of pure gold deposited on a gold film. In the results of FDTD simulations, it can be seen, that the gold antenna can be tuned to have a good mode overlap with the SiV center PL emission. While in practice the gap size was predefined by the spatial dimensions of the nanodimond, the antenna design was simulated for different gap sizes (Figure 3b). As expected, the smaller the gap size g the larger the electric field intensity. Therefore we opted for the aforementioned technical lower limit of the gap size of 150 nm. The shift σ of the emitter

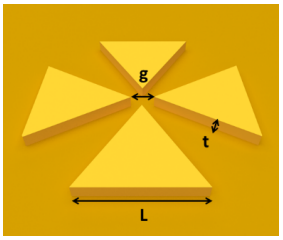

(a)

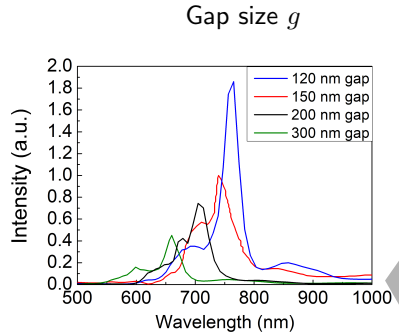

(b)

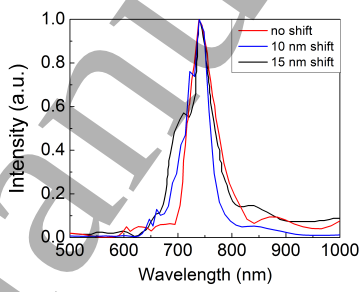

(c)

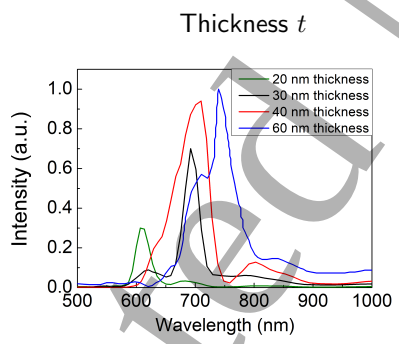

(d)

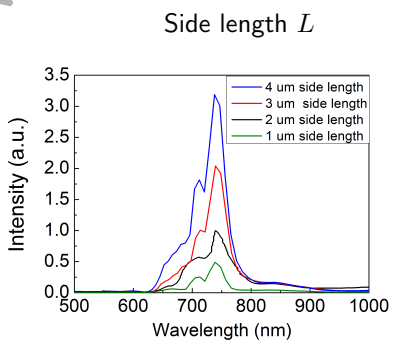

(e)

Figure 3: (a) Schematic of a double bowtie microantenna (on gold substrate) with side length L, thickness t and gap g. (Picture taken from [39]) (b) - (e) FDTD simulations to characterize the double bowtie microantenna. Recorded electric field intensity in the gap as a function of the design parameters: (b) the gap size g between opposite antenna arms; (c) the shift σ of the emitter from the center of the antenna gap; (d) the thickness t of the antenna; (e) the side length L of the antenna triangles. For the FDTD simulations shown in this Figure, one of the mentioned parameters is varied, while the others are fixed at $g = 150\,\text{nm}$; material $=$ gold; $t = 60\,\text{nm}$; $s = 2\,\mu\text{m}$; $\sigma = 0$.

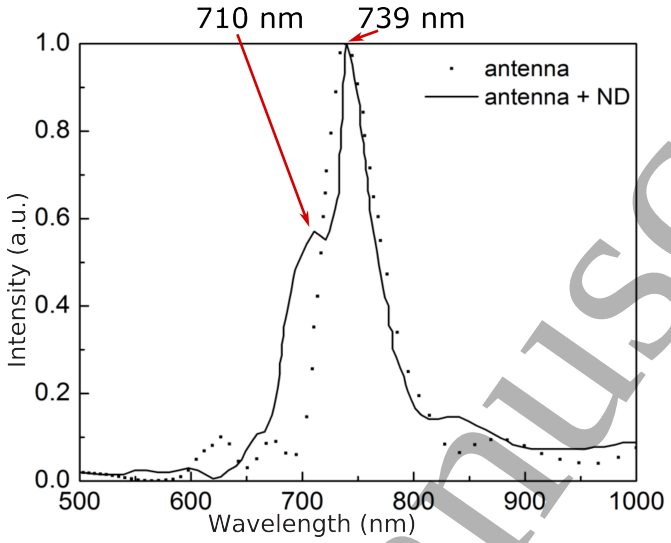

Figure 4: Electric field intensity as a function of wavelength in the gap of a double bowtie microantenna without a nanodiamond (dotted line) and with a nanodiamond (dotted line). Geometrical parameters of the studied antenna: gap $g = 150\,\text{nm}$, side length $L = 2\,\mu\text{m}$, thickness $t = 60\,\text{nm}$.

within the antenna has a negligible effect Figure 3c). With the gap size fixed, the thickness t of the antenna structure has a strong impact on the resonance wavelength of the antenna (Figure 3d). Contrarily, the side length L of the antenna triangles only affects the electric field intensity and not the resonance wavelength (Figure 3e). The final design parameters for the antennas were chosen to have a gap of $g = 150\,\text{nm}$, a side length of $L = 2\,\mu\text{m}$, and a thickness of $t = 60\,\text{nm}$ (see Figure 3a). Further calculations show that the absorption cross section of our antenna structure is $0.46\,\mu\text{m}^2$, which is comparable to similar plasmonic antenna designs reported in the literature [43, 44, 45, 46]. Upon excitation with incident light, an intense electromagnetic hotspot is formed in the microantenna gap, which is expected to excite a nanodiamond containing SiV centers aiming for enhanced fluorescence emission. The spectrum is shown in Figure 4 where we observe two peaks: an intense peak at a center wavelength of 739 nm, exhibiting a large overlap with the SiV center emission wavelength at 738 nm, and an additional mode at a shorter wavelength ($\lambda = 710\,\text{nm}$). The resonance spectrum of the antenna alone shows only one peak at 739 nm. Thus, the additional peak is attributed to the presence of the nanodiamond.

Additional simulations were conducted to demonstrate that the proposed antenna structure is capable of enhancing the emission of SiV centers when placed in the gap. To achieve this, the electric field was measured for a dipole emitter placed on an iridium substrate and compared to the electric field emitted by the dipole positioned at the center of the antenna. The results are shown in Figure 5 where

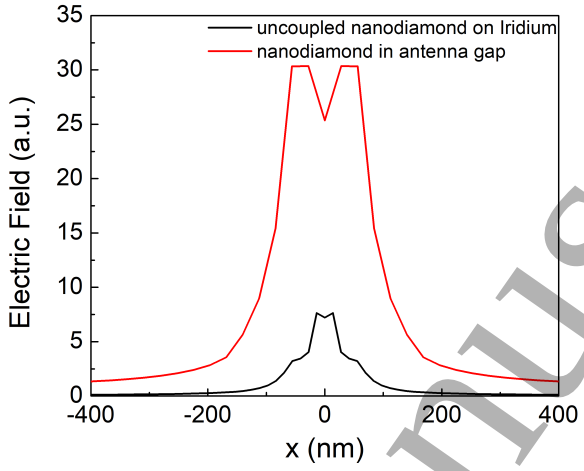

Figure 5: Electric field emitted by an SiV center placed on an iridium substrate (black line) and inside the double bowtie microantenna (red line) as a function of the position x (nm) with respect to the center of the antenna gap. A dipole source emitting at a wavelength of 739 nm is placed at the center of the studied antenna (gap $g = 150$ nm, side length $L = 2$ µm, thickness $t = 60$ nm).

we can see a clear enhancement of the electric field emitted by the dipole.

The structures were then fabricated by electron beam lithography (EBL). A 200 nm layer of polymethyl methyl acrylate (PMMA) is first spin-coated on a sample containing a 60 nm gold layer evaporated on a silicon substrate. A conductive polymer is spin-coated to ensure that no charging effect occurs on the surface. This is followed by e-beam exposure to engrave the desired design on the substrate. Subsequently, the sample is immersed in water to remove the conductive layer, and is then dipped in a methyl isobutyl ketone MIBK solvent followed by isopropanol to remove the exposed areas of the PMMA. A 60 nm layer of gold is then evaporated on the sample. This is followed by a "lift-off" procedure where the sample is dipped in acetone for 2 hours to remove the unexposed regions, resulting in the desired designed pattern, as shown in Figure 6a. An SEM image of the fabricated gold double bowtie antennas is shown in Figure 6b.

4 Nanodiamond Manipulation – Pick-and-Place Technique

After the nanodiamond was pre-selected to exhibit a narrow linewidth and high count rate emission, as described in Section 2, nanodiamond manipulation was performed by the pick-and-place technique, which allows us to transfer nanodiamonds to the

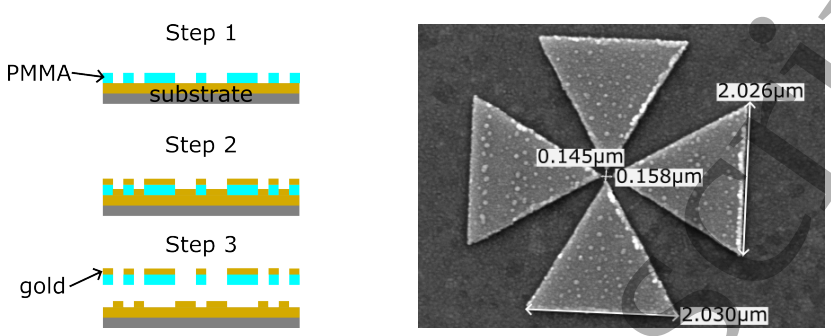

(a) (b)

Figure 6: (a) Schematic of the production process of the gold antenna structure using e-beam lithography (not to scale). Step 1: A PMMA mask is placed on a sample containing a 60 nm gold layer on a silicon substrate, followed by e-beam exposure. Step 2: Deposition of 60 nm of gold. Step 3: Lift off to remove the unexposed areas of the PMMA, resulting in a gold antenna structure on silicon. (b) SEM image of a gold double bowtie microantenna on a gold substrate with target values of $g = 150$ nm and $L = 2$ µm. The actual values obtained after fabrication are indicated in the picture.

sample containing the microantenna structures with the help of a nanomanipulator (schematic in Figure 7a). A nanomanipulator with a tungsten tip (Kleindiek model MM3A-EM; sharpened by a focused ion beam to a radius of curvature = 100 nm) is incorporated inside an SEM (Helios Nanolab600, FEI), operated at 1 kV acceleration voltage to avoid beam damage to the color centers. This allows us to visualize and manipulate the nanodiamonds at the same time. The two samples, one containing 100 nm nanodiamonds on an iridium substrate, and the other one with the gold antennas, are placed inside the SEM. The tip is approached to the surface and gets in contact with the desired pre-characterized nanodiamond. Due to adhesion forces between the tip and the nanodiamond, the latter sticks to the tip as shown in Figure 7b. The tip is then moved to the second sample, carefully approaching the gap of the target microantenna. When the nanodiamond touches the surface , adhesion forces between the nanodiamond and the surface result in separation from the tip and precise placement in the antenna gap, as demonstrated inFigure 7c (the nanodiamond has been colored blue for better visibility in the figure).

The PL spectrum of the nanodiamond in the antenna is measured to identify the effect of the microantenna on its emission. The result is presented in Figure 8a. A $\lambda = 710$ nm long-pass filter is used to eliminate any signal from the laser excitation.

We use a polycristalline nanodiamond hosting several SiV centers. Therefore, the measured photoluminescence intensity stems from SiV centers randomly oriented along different axes. Hence also the SiV centers' dipole orientations are unknown. Due to the pick-and-place process, the probability that the nanodiamond is oriented in exactly the same orientation before and after transfer to the antenna is negligible.

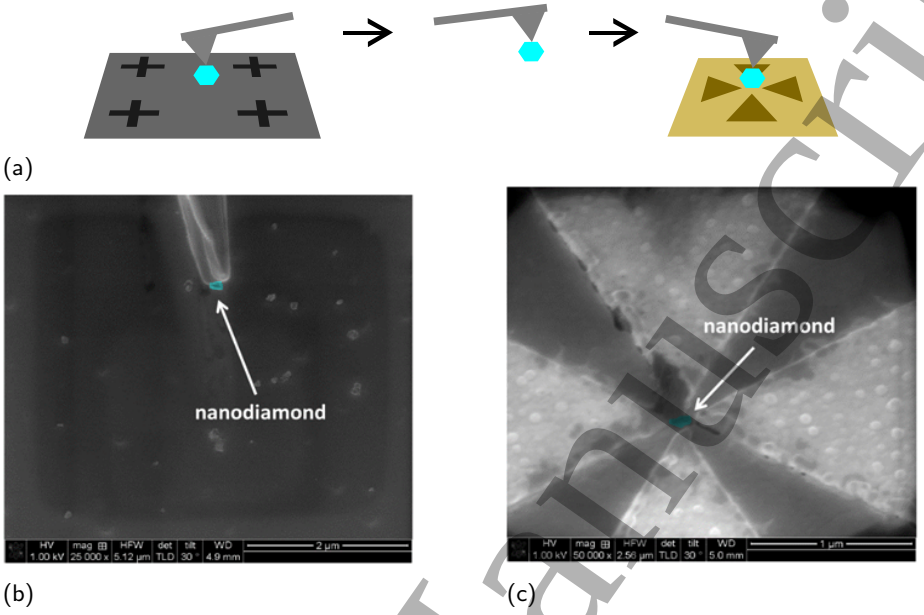

Figure 7: (a) Schematic of the pick-and-place technique for nanodiamond manipulation. SEM images of the (b) nanodiamond (in blue) stuck to the tip and lifted off the substrate (c) nanodiamond deposited in the microantenna gap.

As we excite the SiV with linearly polarized light, we must expect that the excitation efficiency is different before and after transfer [47, 48]. While it is possible to rotate the polarization of the incoming light beam and therefore account for differences of the SiV center dipole orientation in the plane orthogonal to the excitation beam, it is impossible to access differences along the axis of the incoming beam. Furthermore, the antenna is sensitive to the polarization of the photoluminescence light stemming from the SiV center, which should be enhanced. Here the same issues as above apply: the exact polarization state cannot be defined after transfer. We deduced a lower limit accounting for technical imperfections on the measured intensity increase of the recorded photoluminescence of 1.55 ± 0.05 as compared to the nanodiamond located on an iridium surface. Comparing this value to to the simulation results shown in Figure 5 suggests that mentioned polarization issues have a big impact on the measurement.

In addition to the SiV center zero-phonon-line peak at 738.55 nm another peak at a lower wavelength of 726 nm emerges, which is attributed to the antenna resonance mode. To verify this, we convolute the experimental PL spectrum of the nanodiamond measured before placing it in the microantenna gap region Figure 2 with the intensity spectrum of the microantenna obtained by simulations (Figure 4). The result is given in Figure 8b, which is in good agreement with the peak in Figure 8a, confirming that indeed the extra peak is due to the antenna resonance. This is in

accordance with antenna simulations where the geometry of the gap is modified [39] and experiments showing the tuning of a plasmonic antenna with a dielectric nanocrystal [49].

5 Conclusion

In this work, we presented the successful integration of SiV centers in diamond to plasmonic antenna structures. This was achieved by the pick-and-place technique, which was used to transfer a single nanodiamond with SiV centers to the gap of a double bowtie antenna. Optical characterization, sample fabrication as well as numerical FDTD simulations were performed to study the plasmonic structures and hybrid systems. An outstanding agreement was shown between the FDTD simulations of the hybrid system and the photoluminescence measurement of the nanodiamond in the antenna gap. Further work including lifetime and polarization measurements is necessary to give an accurate description of the emission enhancement of the nanodiamond. In addition, the success of the utilized nanomanipulation highlights its potential for interfacing antenna structures and quantum emitters with high precision. Additional future steps will include, but are not limited to saturation and second- order correlation measurements to probe single SiV centers, and consequently quantify the exact Purcell enhancement imposed by the antenna on a single photon emitter. We conclude that careful optimization of various parameters such as the geometry of the antenna, its material, and the position of the emitter in the gap, enables flexible tuning of the resulting PL spectrum of the nanodiamond, which can be adjusted according to the desired application.

Acknowledgements

We want to thank Peter Banzer, University of Graz, for constructive feedback on this manuscript.

Contributions of the authors

SL and NR carried out the investigation and data analysis. CP performed the pick and place process. LG, SM and OAW synthesized the diamond film, AM and AK produced the nanodiamonds from the diamond film. SL, NR, CC and CB co-wrote the initial manuscript. All authors reviewed and edited the manuscript.

ORCID IDs

S. Lindner https://orcid.org/0009-0002-9870-2731

N. Rahbany https://orcid.org/0000-0001-6647-5760

C. Pauly https://orcid.org/0000-0002-6368-2067

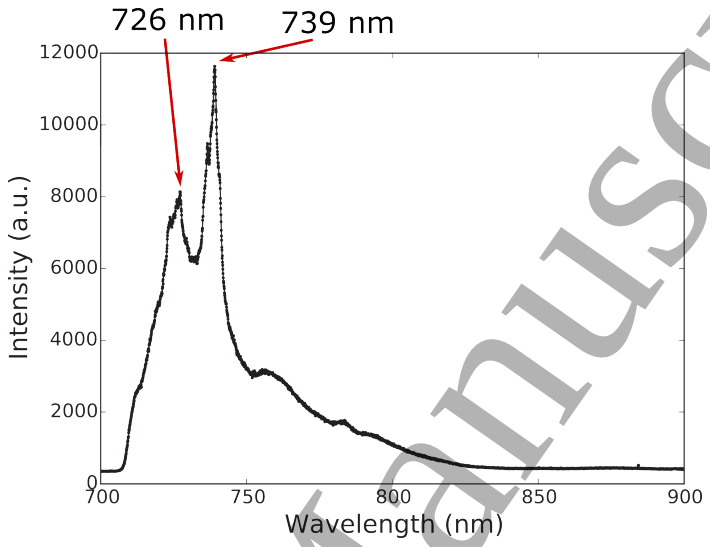

(a)

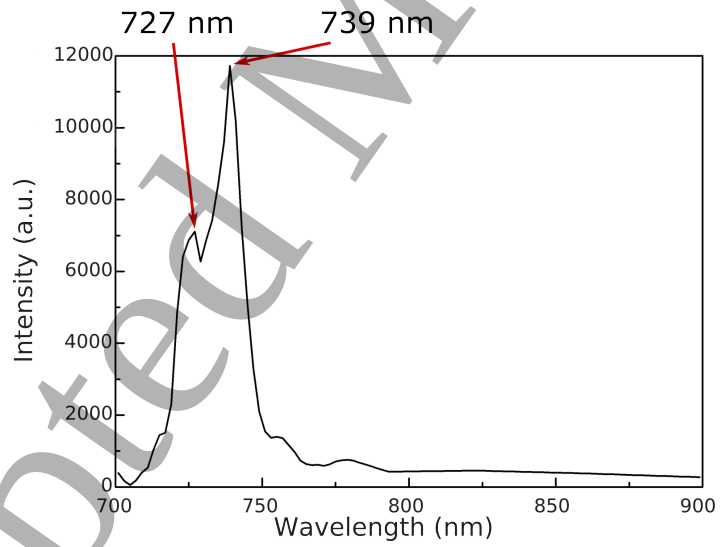

(b)

Figure 8: (a) Experimental PL spectrum of the nanodiamond after placing it in the microantenna., (b) Convolution of the experimental PL spectrum of the nanodiamond with the simulated resonance spectrum of the microantenna.

L. Gines https://orcid.org/0000-0001-9980-054X

S. Mandal https://orcid.org/0000-0001-8912-1439

O. A. Williams https://orcid.org/0000-0002-7210-3004

A. Krueger https://orcid.org/0000-0003-3082-4935

R. Bachelot https://orcid.org/0000-0003-1847-5787

C. Couteau https://orcid.org/0000-0001-7676-3205

C. Becher https://orcid.org/0000-0003-4645-6882

Data availability statement

All data obtained by this study are included in the article.

References

[1] E Togan et al. "Quantum entanglement between an optical photon and a solid-state spin qubit." In: *Nature* 466 (7307 Aug. 2010), pp. 730–734.

[2] M. V. Gurudev Dutt et al. "Quantum Register Based on Individual Electronic and Nuclear Spin Qubits in Diamond". In: *Science* 316 (5829 June 2007), pp. 1312–1316.

[3] I Aharonovich et al. "Diamond-based single-photon emitters". In: *Reports on Progress in Physics* 74 (7 July 2011), p. 076501.

[4] David D. Awschalom et al. "Quantum technologies with optically interfaced solid-state spins". In: *Nature Photonics 2018 12:9* 12 (9 Aug. 2018), pp. 516–527.

[5] C. T. Nguyen et al. "An integrated nanophotonic quantum register based on silicon-vacancy spins in diamond". In: *Physical Review B* 100 (16 Oct. 2019), p. 165428.

[6] Maximilian Ruf et al. "Quantum networks based on color centers in diamond". In: *Journal of Applied Physics* 130 (7 Aug. 2021).

[7] Eva Rittweger et al. "STED microscopy reveals crystal colour centres with nanometric resolution". In: *Nature Photonics 2009 3:3* 3 (3 Feb. 2009), pp. 144–147.

[8] P. C. Maurer et al. "Far-field optical imaging and manipulation of individual spins with nanoscale resolution". In: *Nature Physics 2010 6:11* 6 (11 Sept. 2010), pp. 912–918.

[9] Masfer H. Alkahtani et al. "Fluorescent nanodiamonds: Past, present, and future". In: *Nanophotonics* 7 (8 Aug. 2018), pp. 1423–1453.

[10] Xinyue Wang et al. "Recent applications of nanodiamond quantum biosensors: A review". In: *APL Materials* 11 (9 Sept. 2023).

[11] M. Radtke et al. "Nanoscale sensing based on nitrogen vacancy centers in single crystal diamond and nanodiamonds: achievements and challenges". In: *Nano Futures* 3 (4 Dec. 2019), p. 042004.

[12] Beatrice Rodiek et al. "Experimental realization of an absolute single-photon source based on a single nitrogen vacancy center in a nanodiamond". In: *Optica* 4 (1 2017), p. 71.
[13] Christian Hepp et al. "Electronic Structure of the Silicon Vacancy Color Center in Diamond". In: *Physical Review Letters* 112 (3 Jan. 2014), p. 036405.
[14] Tina Müller et al. "Optical signatures of silicon-vacancy spins in diamond". In: *Nature Communications* 5 (Feb. 2014), p. 3328.
[15] P. Siyushev et al. "Low-temperature optical characterization of a near-infrared single-photon emitter in nanodiamonds". In: *New Journal of Physics* 11 (11 Nov. 2009), p. 113029.
[16] Elke Neu, Mario Agio, and Christoph Becher. "Photophysics of single silicon vacancy centers in diamond: implications for single photon emission". In: *Optics Express* 20 (July 2012), pp. 19956–19971.
[17] Janine Simone Riedrich-Möller et al. "Deterministic coupling of a single silicon-vacancy color center to a photonic crystal cavity in diamond." In: *Nano letters* 14 (9 Aug. 2014), pp. 5281–7.
[18] Tim Schröder et al. "Quantum nanophotonics in diamond [Invited]". In: *Journal of the Optical Society of America B* 33 (4 Apr. 2016), B65.
[19] Julia Benedikter et al. "Cavity-Enhanced Single-Photon Source Based on the Silicon-Vacancy Center in Diamond". In: *Physical Review Applied* 7 (2 2017), p. 024031.
[20] Marina Radulaski et al. "Nanodiamond Integration with Photonic Devices". In: *Laser & Photonics Reviews* 13 (8 Aug. 2019), p. 1800316.
[21] Gregor Bayer et al. "Optical driving, spin initialization and readout of single SiV- centers in a Fabry-Perot resonator". In: *Communications Physics 2023 6:1* 6 (1 Oct. 2023), pp. 1–9.
[22] Sophie W. Ding et al. "High-Q cavity interface for color centers in thin film diamond". In: *Nature Communications* 15 (1 July 2024), p. 6358.
[23] S. Orlanducci et al. "Effects of Au nanoparticles on photoluminescence emission from Si-vacancy in diamond". In: *Chemical Physics Letters* 549 (Oct. 2012), pp. 51–57.
[24] András Szenes et al. "Enhancing Diamond Color Center Fluorescence via Optimized Configurations of Plasmonic Core-Shell Nanoresonator Dimers". In: *ACS Omega* 8 (44 Nov. 2023), pp. 41356–41362.
[25] Dávid Vass et al. "Plasmonically Enhanced Superradiance of Broken-Symmetry Diamond Color Center Arrays Inside Core-Shell Nanoresonators". In: *Nanomaterials* 12 (3 Feb. 2022), p. 352.
[26] Shuo Li et al. "Ag-Diamond Core-Shell Nanostructures Incorporated with Silicon-Vacancy Centers". In: *ACS Materials Au* 2 (2 Mar. 2022), pp. 85–93.
[27] Jie Song et al. "Plasmon-enhanced photoluminescence of Si-V centers in diamond from a nanoassembled metal–diamond hybrid structure". In: *CrystEngComm* 16 (36 July 2014), p. 8356.
[28] András Szenes et al. "Improved emission of SiV diamond color centers embedded into concave plasmonic core-shell nanoresonators". In: *Scientific Reports 2017 7:1* 7 (1 Oct. 2017), pp. 1–10.

[29] András Szenes et al. "Enhancing Diamond Color Center Fluorescence via Optimized Plasmonic Nanorod Configuration". In: *Plasmonics* 12 (4 Aug. 2017), pp. 1263–1280.
[30] Andrew M. Boyce et al. "Plasmonic Diamond Membranes for Ultrafast Silicon Vacancy Emission". In: *Nano Letters* 24 (12 Mar. 2024), pp. 3575–3580.
[31] Alexey M Romshin et al. "Effectively enhancing silicon-vacancy emission in a hybrid diamond-in-pit microstructure". In: *Laser Physics Letters* 20 (1 Jan. 2023), p. 015206.
[32] Boaz Lubotzky et al. "Room-Temperature Fiber-Coupled Single-Photon Sources based on Colloidal Quantum Dots and SiV Centers in Back-Excited Nanoantennas". In: *Nano Letters* 24 (2 Jan. 2024), pp. 640–648.
[33] Michael Barth et al. "Controlled coupling of NV defect centers to plasmonic and photonic nanostructures". In: *Journal of Luminescence* 130 (9 Sept. 2010), pp. 1628–1634.
[34] Sarah Christina Barbara Lindner. "Towards integrated single-photon sources exploiting inhomogeneous spectral properties of the silicon-vacancy center in nanodiamonds". In: *Doctoral dissertation, Saarland University* (2018).
[35] Oliver A. Williams and Miloš Nesládek. "Growth and properties of nanocrystalline diamond films". In: *Phys. status solidi* 203 (13 Oct. 2006), pp. 3375–3386.
[36] Sarah Lindner et al. "Strongly inhomogeneous distribution of spectral properties of silicon-vacancy color centers in nanodiamonds". In: *New Journal of Physics* (2018), p. 115002.
[37] P. Biagioni et al. "Cross Resonant Optical Antenna". In: *Physical Review Letters* 102 (25 June 2009), p. 256801.
[38] Paolo Biagioni, Jer-Shing Huang, and Bert Hecht. "Nanoantennas for visible and infrared radiation". In: *Reports on Progress in Physics* 75 (2 Feb. 2012), p. 024402.
[39] Nancy Rahbany et al. "Integrated plasmonic double bowtie / ring grating structure for enhanced electric field confinement". In: *Nanospectroscopy* 1 (1 2015), pp. 61–66.
[40] Nancy Rahbany et al. "Plasmon–emitter interaction using integrated ring grating–nanoantenna structures". In: *Nanotechnology* 28 (18 Apr. 2017), p. 185201.
[41] Edward D Palik. *Handbook of optical constants of solids*. Vol. 3. Academic press, 1998.
[42] A. M. Zaitsev. *Optical properties of diamond: a data handbook*. 2001.
[43] Hamidreza Siampour and Yaping Dan. "Si nanowire phototransistors at telecommunication wavelengths by plasmon-enhanced two-photon absorption". In: *Optics Express, Vol. 24, Issue 5, pp. 4601-4609* 24 (5 Mar. 2016), pp. 4601–4609.
[44] Wounjhang Park. "Optical interactions in plasmonic nanostructures". In: *Nano Convergence* 1 (1 Dec. 2014), pp. 1–27.
[45] Linhan Lin and Yuebing Zheng. "Optimizing plasmonic nanoantennas via coordinated multiple coupling". In: *Scientific Reports 2015 5:1* 5 (1 Oct. 2015), pp. 1–11.

[46] Akash Srivastava and Devendra Chack. "Plasmonic Nanoantenna Array-Based Sensor for Air Parameters Monitoring Purpose". In: *Plasmonics* (Aug. 2024), pp. 1–12.

[47] Lachlan J. Rogers et al. "Multiple intrinsically identical single-photon emitters in the solid state." In: *Nature communications* 5 (Jan. 2014), p. 4739.

[48] Yan Liu et al. "Fluorescence Polarization Switching from a Single Silicon Vacancy Colour Centre in Diamond". In: *Scientific Reports 2015 5:1* 5 (1 July 2015), pp. 1–9.

[49] Yury Alaverdyan et al. "Spectral tunability of a plasmonic antenna with a dielectric nanocrystal". In: *Optics Express* 19 (19 Sept. 2011), p. 18175.